Phenylcyanamido Ligand Building Molecular, 1-D, and 2-D Systems − Syntheses, Crystal Structures and Magnetic Properties

Albert Escuer,[a] Núria Sanz,[a] Franz A. Mautner,[b] and Ramon Vicente*[a]

Keywords: Manganese / Magnetic properties / Phenylcyanamido ligands / Bridging ligands

Several Mn^{II} compounds have been synthesised with the phenylcyanamido ligand, C_6H_5–NCN^-, and characterised by means of single crystal X-ray structure determination. The reported compounds show a wide variety of nuclearity: mononuclear, dinuclear, 1-D, and 2-D compounds are present in which the phenylcyanamido anion ($pcyd^-$) acts as a bridging ligand. The mononuclear compound $[Mn(pcyd)_2(phen)_2]$ (**1**) crystallises in the orthorhombic system, *Pbcn* space group; dinuclear compound $[\{Mn(pcyd)(phen)(MeOH)\}_2(\mu_{1,3}\text{-}pcyd)_2]$ (**2**) crystallises in the monoclinic system, *C*2/*c* space group; 1-D chain $[Mn(4\text{-}bzpy)_2(\mu_{1,3}\text{-}pcyd)_2]_n$·MeOH (**3**·MeOH) crystallises in the triclinic system, $P\bar{1}$ space group; 2-D network $[Mn(\mu_{1,3}\text{-}pcyd)_2(\mu\text{-}4,4'\text{-}bpy)]_n$·MeOH (**4**·MeOH) crystallises in the monoclinic system, C2 space group. Susceptibility measurements on compounds **2**–**4** reveal moderate AF coupling in all cases.

Introduction

In the last few years, a wide variety of bridging ligands have been used to promote the magnetic interaction between transition metal ions in polynuclear systems. In this sense, the anions azido[1] and dicyanamido[2] have generated a plethora of new polynuclear compounds ranging from dinuclear to 3D with different architectures. The study of the magnetic behaviour of these compounds has made for fast growth in the field molecular magnetism. However, the X-phenylcyanamido ligands (X-$pcyd^-$), Scheme 1, have practically been forgotten[3,4] as superexchange mediators in spite of the similarities with the azido or dicyanamido ligands. The $XPh-NCN^-$ group is electronically similar to the azido ligand (N_3^-), and it is reasonable to expect similar coordination modes. On the other hand, the nitrile group approaches the coordination properties of those observed for the dicyanamido ligand (mainly for M−N−C and M−N bond parameters).[2,5]

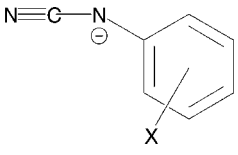

Scheme 1

With the aim of exploring the magnetic and synthetic possibilities of the R-phenylcyanamido ligands, we have recently published[5] the syntheses and structural characterisation of several representative Mn^{II} derivatives: the mononuclear compound $[Mn(3\text{-}Clpcyd)_2(H_2O)_2(4\text{-}bzpy)_2]$; the dinuclear ones $[\{Mn(3\text{-}Clpcyd)(2,2'\text{-}bpy)(S)\}_2(\mu_{1,3}\text{-}3\text{-}Clpcyd)_2]$, S = MeOH or EtOH; the 1-D $[Mn(2,2'\text{-}bpy)(\mu_{1,3}\text{-}4\text{-}Clpcyd)_2]_n$ and the 2-D $[Mn(\mu_{1,3}\text{-}3\text{-}Fpcyd)_2(\mu\text{-}4,4'\text{-}bpy)]_n$, in which 4-bzpy is 4-benzoylpyridine, 2,2′-bpy and 4,4′-bpy corresponds to the 2,2′- and 4,4′-bipyridyls. This series of compounds was obtained by using different X-phenylcyanamido derivatives: 3-$Clpcyd^-$, 4-$Clpcyd^-$ and 3-$Fpcyd^-$ are the 3-chloro-, 4-chloro-, or 3-fluorophenylcyanamido ligands, respectively. Magnetic measurements on the polynuclear $\mu_{1,3}$-X-$pcyd^-$ compounds revealed moderate AF coupling for all of them. This coupling lies in an intermediate position between the typical magnitude of the coupling induced by $\mu_{1,3}$ azido and $\mu_{1,5}$ dicyanamido bridges. MO calculations have evaluated the influence of the chair distortion of the $Mn-(NCN)_2-Mn$ unit, the effect of the halo substituent in the *para* position and the torsion effect of the phenyl rings on the superexchange interaction, and the theoretical results have been correlated with the experimental data.

In this paper, bearing in mind that the number of compounds is still low, we extend the study to the coordination compounds derived from the X-phenylcyanamido ligands by reporting the use of *only* the phenylcyanamido anion ($pcyd^-$), to synthesise a new series of $[Mn(pcyd)_2(L)_n]$ derivatives which show different nuclearities and dimensionalities. Successful syntheses and structural characterisation have been carried out for several representative complexes,

[a] Departament de Química Inorgànica, Universitat de Barcelona, c/ Martí Franquès 1−11, 08028 Barcelona, Spain
Fax: (internat.) +34-(0)93-4907725
E-mail: ramon.vicente@qi.ub.es
[b] Institut für Physikalische und Theoretische Chemie, Technische Universität Graz,
8010 Graz, Austria
E-mail: Mautner@ptc.tu-graz.ac.at

with formulae $[Mn(pcyd)_2(phen)_2]$ (**1**), $[\{Mn(pcyd)(phen)(MeOH)\}_2(\mu_{1,3}\text{-pcyd})_2]$ (**2**), $[Mn(4\text{-bzpy})_2(\mu_{1,3}\text{-pcyd})_2]\cdot MeOH$ (**3**·MeOH) and $[Mn(\mu_{1,3}\text{-pcyd})_2(\mu\text{-}4,4'\text{-bpy})]_n\cdot MeOH$ (**4**·MeOH) where 4-bzpy is 4-benzoylpyridine, 4,4′-bpy corresponds to 4,4′-bipyridyl and phen is 1,10-phenanthroline. These compounds were obtained by reaction in alcoholic media of manganese salts with the corresponding pyridinic or bipyridinic ligands and the deprotonated phenylcyanamide. The X-ray crystal structure determination reveals a wide variety of topologies and supramolecular arrangements: compound **1** is a mononuclear complex; compounds **2** a dinuclear complex bridged by double phenylcyanamido ligands, giving a supramolecular 1-D system by means of hydrogen bonds; compound **3**·MeOH is a chain of manganese atoms linked by double phenylcyanamido bridges. Finally, compound **4**·MeOH is a 2-D system formed by the crossing of phenylcyanamido and 4,4′-bpy chains. This paper gives the second structural set of data for polynuclear phenylcyanamide bridged derivatives with Mn^{II} as the central atom, together with a set of new experimental variable temperature susceptibility data for the $\mu_{1,3}$-X-pcyd$^-$ superexchange mediator.

Magnetic measurements for compounds **2**−**4** reveal a moderate AF coupling which lies in an intermediate position between the typical values of the coupling induced by $\mu_{1,3}$-azido and $\mu_{1,5}$-dicyanamido bridges. The obtained coupling constants are in accordance with the general rules for the $\mu_{1,3}$ coordination mode of pcyd$^-$ ligands discussed in the previous paper.[5]

Results and Discussion

Infrared Spectra: Neutral pcydH shows a characteristic IR ν(NCN) stretching absorption over a short wavenumber range (2225−2249 cm^{-1}), which shifts down to ca. 2120 cm^{-1} for deprotonated pcyd$^-$, suggesting a lower contribution of the resonance form containing the nitrile fragment. *N*-nitrile-coordinated X-pcyd$^-$ ligands, exhibit intermediate positions (always lower than 2200 cm^{-1}), with a dependence on the nature of the metallic centre and the number of halo groups.[3] For pcyd$^-$, the signal appears at 2108 cm^{-1} for **1** (only *N*-nitrile-coordinated pcyd$^-$ ligand), at 2168−2136 cm^{-1} for **2** (containing the two $\mu_{1,3}$-pcyd and *N*-nitrile pcyd$^-$ coordination modes) and at 2164 and 2133 cm^{-1} for **3** and **4,** respectively (containing the two $\mu_{1,3}$-X-pcyd$^-$ coordination modes). The structurally characterised $\mu_{1,3}$ copper dimer $[\{Cu(pcyd)(2,2'\text{-bpy})\}_2(\mu_{1,3}\text{-pcyd})_2]$[6] is in reasonable agreement with this assignment: it exhibits two similar absorptions at 2175 and 2103 cm^{-1}. In the mononuclear compound with the 3-Clpcyd$^-$ ligand $[Mn(3\text{-Clpcyd})_2(H_2O)_2(4\text{-bzpy})_2]$ the signal appears at 2108 cm^{-1} (only *N*-nitrile-coordinated pcyd$^-$ ligand) and at 2155−2132 cm^{-1} and 2159−2133 cm^{-1} in the dinuclear ones $[\{Mn(3\text{-Clpcyd})(2,2'\text{-bpy})(S)\}_2(\mu_{1,3}\text{-3-Clpcyd})_2]$, S = MeOH or EtOH, respectively (containing the two $\mu_{1,3}$-pcyd$^-$ and *N*-nitrile pcyd$^-$ coordination modes).[5] The wavenumber sequence for the ν(NCN) stretching absorption seems then to be pcydH > $\mu_{1,3}$-X-pcyd > *N*-nitrile coordination or anionic X-pcyd$^-$. The limited data for Mn^{II} derivatives suggest the above order, but further experimental data are required to obtain a general assignment.

Description of the Structure of $[Mn(pcyd)_2(phen)_2]$ (1): This compound consists of monomeric units in which the terminal pcyd$^-$ ligands adopt a *cis* arrangement around the central Mn^{II} ion (Figure 1). Selected bond parameters are given in Table 1.

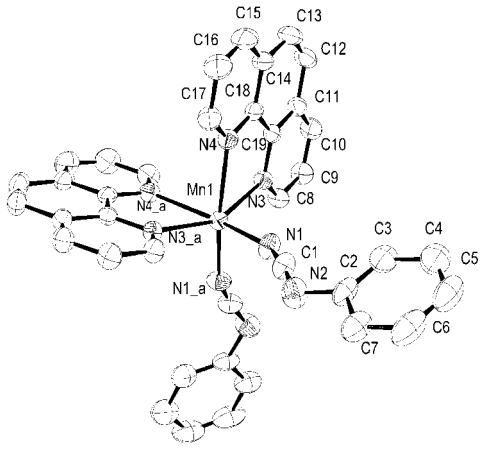

Figure 1. Labelled plot of $[Mn(pcyd)_2(phen)_2]$ (**1**)

Table 1. Selected bond lengths [Å] and angles [°] for $[Mn(pcyd)_2(phen)_2]$ (**1**)

Mn(1)−N(1)	2.131(3)	Mn(1)−N(3)	2.321(2)
Mn(1)−N(4)	2.314(2)		
N(1)−Mn(1)−N(4_a)[a]	159.5(1)	N(3)−Mn(1)−N(4)	71.3(1)
N(1)−Mn(1)−N(3)	107.2(1)	N(3)−Mn(1)−N(3_a)	155.2(1)
N(1)−Mn(1)−N(4)	90.8(1)	N(3)−Mn(1)−N(4_a)	90.1(1)
N(1)−Mn(1)−N(3_a)	88.9(1)	N(4)−Mn(1)−N(4_a)	84.1(1)
N(1)−Mn(1)−N(1_a)	100.4(1)		
N(1)−C(1)	1.154(5)	C(1)−N(2)	1.299(6)
N(2)−C(2)	1.388(6)		
Mn(1)−N(1)−C(1)	158.8(5)	N(1)−C(1)−N(2)	171.5(5)
C(1)−N(2)−C(2)	121.7(4)		

[a] Symmetry codes: _a: $-x, y, -z + 1/2$

The Mn^{2+} ion shows a strongly distorted octahedral environment imposed by the rigidity of the 1,10-phenantroline ligands. The pcyd$^-$ ligands are coordinated to the Mn atom by the nitrile N atoms. There are two kinds of bond Mn−N distances: a short distance of 2.131(3) Å between the Mn^{II} ion and the nitrile N atoms, and longer distances to the N(phen) atoms: Mn(1)−N(3) 2.312(2) Å and Mn(1)−N(4) 2.314(2) Å. The most distorted bond angles around the Mn atom are N(3)−Mn−N(4), 71.3(1)°, N(1)−Mn−N(1_a), 100.4(1)° and N(4)−Mn−N(4_a), 84.1(1)°. The coordination of the monodentate phenylcyanamido ligand to the manganese atom is not linear with a Mn(1)−N(1)−C(1) bond angle of 158.8(5)°.

The NCN unit is practically linear with a N(1)−C(1)−N(2) angle of 171.5°. NCN is asymmetric, with bond lengths of N(1)−C(1) = 1.154(5) Å and C(1)−N(2) =

1.299(6) Å. The cyanamido unit is practically coplanar with the phenyl group of the pcyd$^-$ ligand and shows a C(1)−N(2)−C(2) bond angle of 121.7(4)°.

Description of the Structure of [{Mn(pcyd)(phen)(MeOH)}$_2$($\mu_{1,3}$-pcyd)$_2$] (2): The structure consists of centrosymmetric dinuclear Mn units linked by double end-to-end phenylcyanamido bridges (Figure 2). Selected bond parameters are given in Table 2.

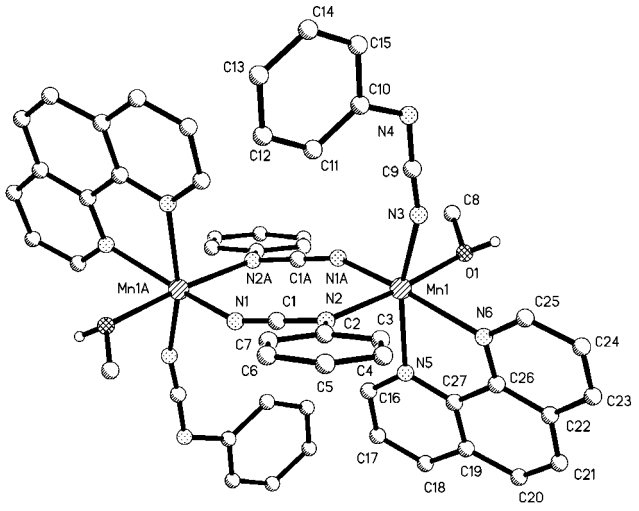

Figure 2. Labelled plot of [{Mn(pcyd)(phen)(MeOH)}$_2$($\mu_{1,3}$-pcyd)$_2$] (**2**)

Table 2. Selected bond lengths [Å] and angles [°] for [{Mn(pcyd)(phen)(MeOH)}$_2$($\mu_{1,3}$-pcyd)$_2$] (**2**)

Mn(1)−O(1)	2.235(2)	Mn(1)−N(5)	2.306(2)
Mn(1)−N(2)	2.278(2)	Mn(1)−N(6)	2.300(2)
Mn(1)−N(3)	2.140(2)	Mn(1)−N(1A)	2.166(2)
O(1)−Mn(1)−N(2)	175.1(1)	N(2)−Mn(1)−N(3)	91.2(1)
O(1)−Mn(1)−N(3)	87.4(1)	N(2)−Mn(1)−N(5)	92.8(1)
O(1)−Mn(1)−N(5)	89.8(1)	N(2)−Mn(1)−N(6)	105.5(1)
O(1)−Mn(1)−N(6)	79.2(1)	N(2)−Mn(1)−N(1A)	88.5(1)
O(1)−Mn(1)−N(1A)[a]	87.4(1)	N(5)−Mn(1)−N(6)	72.1(1)
N(3)−Mn(1)−N(5)	163.7(1)	N(5)−Mn(1)−N(1A)	91.4(1)
N(3)−Mn(1)−N(6)	91.6(1)	N(6)−Mn(1)−N(1A)	158.6(1)
N(3)−Mn(1)−N(1A)	104.6(1)		
N(1)−C(1)	1.167(3)	N(3)−C(9)	1.160(3)
C(1)−N(2)	1.296(3)	C(9)−N(4)	1.289(3)
C(2)−N(2)	1.413(3)	C(10)−N(4)	1.404(3)
Mn(1A)−N(1)−C(1)	156.2(2)	Mn(1)−N(3)−C(9)	160.3(1)
N(1)−C(1)−N(2)	176.4(2)	N(3)−C(9)−N(4)	176.5(2)
C(1)−N(2)−Mn(1)	113.2(1)	C(9)−N(4)−C(10)	117.2(2)
Mn(1)−N(2)−C(2)	129.2(1)		
C(2)−N(2)−C(1)	117.0(2)		

[a] Symmetry codes: (A) $-x$, $-y$, $-z+1$.

The six coordination sites around the Mn atoms are occupied by the two N atoms of one phen ligand, one nitrile N atom of the terminal pcyd$^-$ ligand, one nitrile and one amido nitrogen atoms of the two bridging cyanamido ligands and one O atom of the solvent molecule (methanol). The linked phen and the variety of ligands distorts the coordination polyhedron of the Mn atom: bond angles ranging between 72.1(1)° for N(5)−Mn(1)−N(6) and 105.5(1)° for N(2)−Mn(1)−N(6) are found. The different nature of the N atoms of the phenylcyanamido ligand also induces different bond parameters in the bridging region: Mn(1)−N(1) takes the value of 2.278(2) Å whereas Mn(1)−N(1A) is only 2.166(2) Å. Mn−*N*−C bond angles are also different, being Mn(1A)−N(1)−C(1) 156.2(2)° in contrast with Mn(1)−N(2)−C(1), which takes the value of 113.2(1)°. As occurs in **1**, the monodentate phenylcyanamido ligands coordinate to the manganese atom in a quasi-linear arrangement, with a Mn(1)−N(3)−C(9) bond angle of 160.3(1)°.

The C−N−C angles between the cyanamido and the phenyl groups are similar for the terminal and the bridging ligands: 117.2(2)° and 117.0(2)°, respectively. The Mn−(NCN)$_2$−Mn subunit shows a chair distortion similar to those often found in similar systems with double azido bridges.[1] This means that the two −NCN− groups are in the same plane with the manganese atoms placed 0.403(1) Å out of the main plane. The torsion angle between the plane determined by the two −NCN− groups and the N(2)−Mn(1)−N(1A) plane is 14.7(1)°. The pcyd$^-$ ligand is practically planar with a minor torsion of 4.1(2)° between the bond direction N(2)−C(2) and the (NCN)$_2$ plane. The phenylcyanamido ligand is placed out of the main (NCN)$_2$ plane, which forms an acute angle of 15.7(1)° with the N(2)−C(2) bond direction. The Mn···Mn intradimer distance is 5.479(1) Å.

The dinuclear units generate a supramolecular one-dimensional H-bonded system by means of the OH group of the coordinated methanol molecules, O(1) atom, and the N(4) atoms of the terminal pcyd$^-$ ligands. Two of these H bonds appear between each dinuclear unit, giving a structurally alternating 1-D system (Figure 3). The N(4)−O(1) distance is 2.727(2) Å and the bond angle O(1)−H(1)−N(4) has a value of 178(3)°.

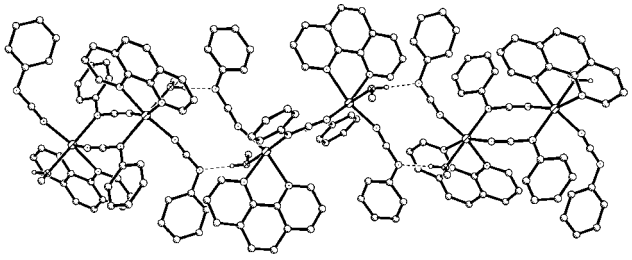

Figure 3. Hydrogen bond chain in compound **2**

Description of the Structure of [Mn(4-bzpy)$_2$($\mu_{1,3}$-pcyd)$_2$]·MeOH (3·MeOH): Selected bond parameters are given in Table 3. The structure consists of a one-dimensional Mn system where the coordination environment around the Mn atoms includes two N atoms of *trans*-4-bzpy ligands and four N atoms of bridging pcyd$^-$ ligands. The compound crystallizes with one MeOH molecule per formula unit.

Table 3. Selected bond lengths [Å] and angles [°] for $[Mn(4\text{-bzpy})_2(\mu_{1,3}\text{-pcyd})_2]\cdot MeOH$ (**3**·MeOH)

Mn(1)−N(1)	2.168(2)	Mn(1)−N(4)	2.272(3)
Mn(1)−N(2)	2.305(3)	Mn(1)−N(5)	2.329(3)
Mn(1)−N(3)	2.195(2)	Mn(1)−N(6)	2.275(3)
N(1)−Mn(1)−N(3)	175.5(1)	N(3)−Mn(1)−N(2)	95.7(1)
N(1)−Mn(1)−N(2)	86.4(1)	N(3)−Mn(1)−N(4)	88.3(1)
N(1)−Mn(1)−N(4)	89.0(1)	N(3)−Mn(1)−N(5)	85.9(1)
N(1)−Mn(1)−N(5)	90.5(1)	N(3)−Mn(1)−N(6)	86.5(1)
N(1)−Mn(1)−N(6)	97.4(1)	N(4)−Mn(1)−N(5)	88.2(1)
N(2)−Mn(1)−N(4)	170.2(1)	N(4)−Mn(1)−N(6)	95.9(1)
N(2)−Mn(1)−N(5)	83.2(1)	N(5)−Mn(1)−N(6)	171.5(1)
N(2)−Mn(1)−N(6)	93.9(1)		
N(1)−C(1)	1.166(4)	N(3)−C(8)	1.165(4)
C(1)−N(2_a)[a]	1.300(4)	C(8)−N(4_b)	1.301(4)
N(2)−C(2)	1.413(4)	N(4)−C(9)	1.411(4)
Mn(1)−N(1)−C(1)	142.3(2)	Mn(1)−N(3)−C(8)	141.9(2)
N(1)−C(1)−N(2_a)	175.2(3)	N(3)−C(8)−N(4_b)	175.5(3)
C(1)−N(2_a)−Mn(1_a)	109.0(2)	C(8)−N(4_b)−Mn(1_b)	110.5(2)
Mn(1)−N(2)−C(2)	132.3(2)	Mn(1)−N(4)−C(9)	128.7(2)
C(2)−N(2)−C(1_a)	116.6(2)	C(9)−N(4)−C(8_b)	117.9(3)

[a] Symmetry codes: _a: $-x, -y, -z + 1$; _b: $-x + 1, -y, -z + 1$.

Double cyanamido bridges link the Mn atoms, giving a *trans* chain (Figure 4). The bond parameters in the bridging region show different bond lengths for the Mn−N(nitrile) and the Mn−N(amide) unions: Mn(1)−N(1), 2.168(2) Å and Mn(1)−N(3), 2.195(2) Å; Mn(1)−N(2), 2.305(3) Å, and Mn(1)−N(4), 2.272(3) Å. The bond angle Mn(1_a)−N(2_a)−C(1), 109.0(2)° is clearly smaller than Mn(1)−N(1)−C(1), 142.3(2)°. The Mn−$(NCN)_2$−Mn subunits show an important chair distortion: for the Mn(1)−[N(1)−C(1)−N(2)]$_2$−Mn(1_a) ring the Mn atoms are placed 0.979(1) Å out of the $(NCN)_2$ main plane and there is a dihedral angle of 37.0(1)° between the N(1)−Mn(1)−N(2) plane and the main $(NCN)_2$ plane. In this case the deviation of the phenyl groups, given by the acute angle between the bond directions N(2)−C(2) or N(4)−C(9) and the $(NCN)_2$ plane are only 9.6(2) and 7.2(2)°, respectively. The Mn atoms are placed 0.048 Å out of the $(NCN)_2$ plane in the Mn(1_b)−[N(3)−C(8)−N(4)]$_2$−Mn(1) dinuclear unit. The dihedral angle between N(3)−Mn(1)−N(4) and the main $(NCN)_2$ plane is 36.1°. The Mn···Mn intrachain distance is 5.328(1) Å, whereas the minimum interchain Mn···Mn distance is 8.520(1) Å.

Description of the Structure of $[Mn(\mu_{1,3}\text{-pcyd})_2(\mu\text{-}4,4'\text{-bpy})]_n\cdot MeOH$ (4·MeOH): The use of 4,4′-bpy determines a *trans*-octahedral arrangement around the Mn atoms (Figure 5). Selected bond parameters are given in Table 4.

The compound crystallises with a MeOH molecule per formula unit. The coordination sites around the manganese atom are occupied by two *trans* N atoms of two bridging 4,4′-bpy ligands and by four bridging $pcyd^-$ ligands. The structure may then be described as a two-dimensional sys-

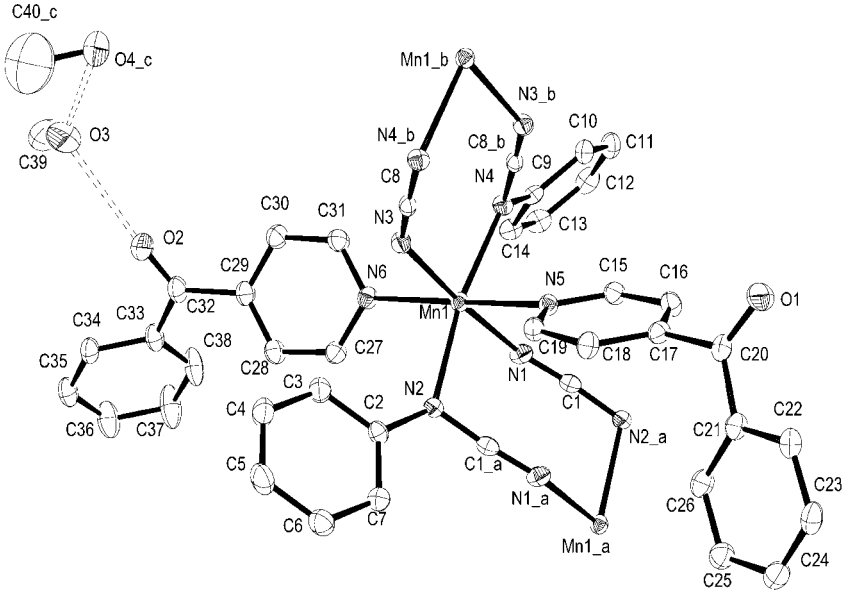

Figure 4. ORTEP plot of $[Mn(4\text{-bzpy})_2(\mu_{1,3}\text{-pcyd})_2]\cdot MeOH$ (**3**·MeOH) with thermal ellipsoids at the 40% probability level

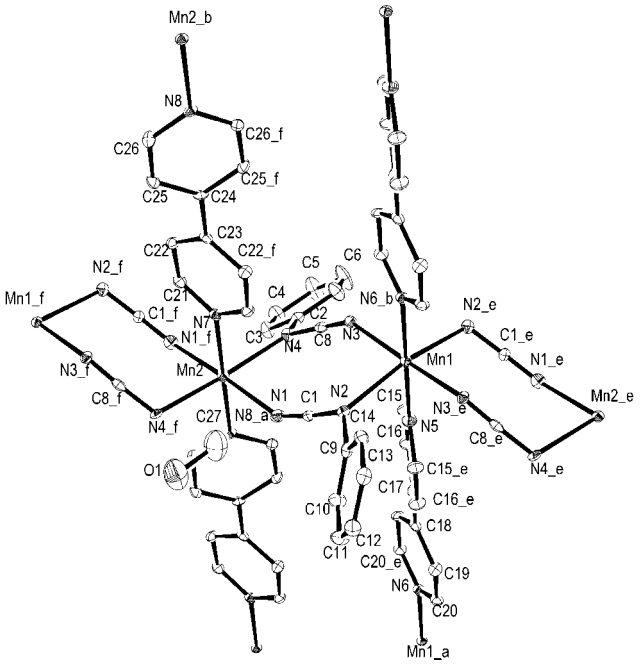

Figure 5. ORTEP plot of the basic unit of $[Mn(\mu_{1,3}\text{-pcyd})_2(\mu\text{-}4,4'\text{-bpy})]_n\cdot$MeOH (**4**·MeOH) with thermal ellipsoids at the 50% probability level

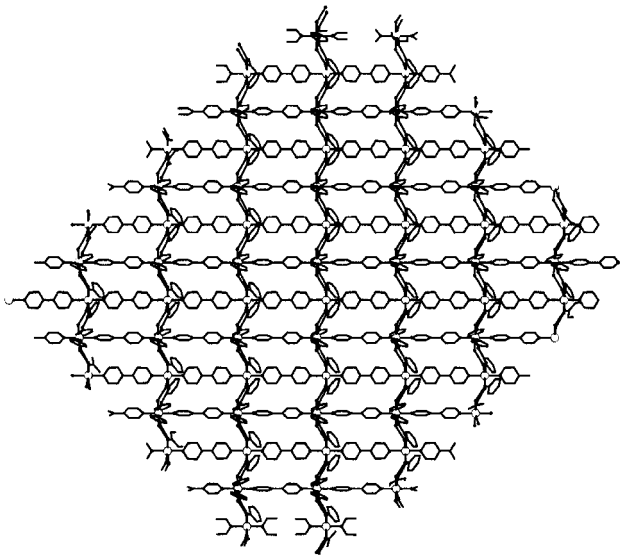

Figure 6. View of the 2-D arrangement of **4**·MeOH by means of the pcyd and 4,4′-bipy bridging ligands

tem with 4,4′-bpy-Mn chains crossed by Mn-pcyd chains (Figure 6).

The bond lengths in the bridging region again show a clear difference between nitrile and amide N atoms of the ligand: bond lengths for Mn(1)−N(3) and Mn(2)−N(1) are 2.187(4) Å and 2.173(3) Å whereas Mn(1)−N(2) and Mn(2)−N(4) are 2.315(4) Å and 2.327(4) Å, respectively. Bond angles related to the nitrile N atom Mn(1)−N(3)−C(8), 148.9(5)° and Mn(2)−N(1)−C(1), 142.3(4)° are larger than the angles related to the amide N atom Mn(1)−N(2)−C(1), 111.7(3)° and Mn(2)−N(4)−C(8), 111.2(3)°. As occurs for the above compounds, Mn−$(NCN)_2$−Mn subunits show a clear chair distortion with the Mn atoms placed 0.808(1)−0.942(1) Å out of the cyanamido plane. A dihedral angle of 30.6(2)−34.3(2)° is found between the $(NCN)_2$ planes and N(1)−Mn(2)−N(4)

Table 4. Selected bond lengths [Å] and angles [°] for $[Mn(\mu_{1,3}\text{-pcyd})_2(\mu\text{-}4.4'\text{-bpy})]_n\cdot$MeOH (**4**·MeOH)

Mn(1)−N(5)	2.350(7)	Mn(2)−N(7)	2.301(7)
Mn(1)−N(6_b)[a]	2.279(7)	Mn(2)−N(8_a)	2.312(7)
Mn(1)−N(2)	2.315(4)	Mn(2)−N(1)	2.173(3)
Mn(1)−N(3)	2.187(4)	Mn(2)−N(4)	2.327(4)
N(5)−Mn(1)−N(6_b)	180.0(6)	N(7)−Mn(2)−N(8_a)	180.0(1)
N(5)−Mn(1)−N(2)	87.6(1)	N(7)−Mn(2)−N(1)	91.7(1)
N(5)−Mn(1)−N(3)	92.4(2)	N(7)−Mn(2)−N(4)	82.8(1)
N(5)−Mn(1)−N(2_e)	87.6(1)	N(7)−Mn(2)−N(1_f)	91.7(1)
N(5)−Mn(1)−N(3_e)	92.4(2)	N(7)−Mn(2)−N(4_f)	82.8(1)
N(6_b)−Mn(1)−N(2)	92.4(1)	N(8_a)−Mn(2)−N(1)	88.3(1)
N(6_b)−Mn(1)−N(3)	87.6(2)	N(8_a)−Mn(2)−N(4)	97.2(1)
N(6_b)−Mn(1)−N(2_e)	92.4(1)	N(8_a)−Mn(2)−N(1_f)	88.3(1)
N(6_b)−Mn(1)−N(3_e)	87.6(2)	N(8_a)−Mn(2)−N(4_f)	97.2(1)
N(2)−Mn(1)−N(3)	84.8(1)	N(1)−Mn(2)−N(4)	88.8(1)
N(2)−Mn(1)−N(2_e)	175.2(2)	N(1)−Mn(2)−N(1_f)	176.7(2)
N(2)−Mn(1)−N(3_e)	95.4(1)	N(1)−Mn(2)−N(4_f)	91.6(1)
N(3)−Mn(1)−N(2_e)	95.4(1)	N(4)−Mn(2)−N(1_f)	91.6(1)
N(3)−Mn(1)−N(3_e)	175.2(1)	N(4)−Mn(2)−N(4_f)	165.3(1)
N(2_e)−Mn(1)−N(3_e)	84.8(1)	N(1_f)−Mn(2)−N(4_f)	88.8(1)
N(3)−C(8)	1.175(6)	N(1)−C(1)	1.162(6)
C(8)−N(4)	1.278(6)	C(1)−N(2)	1.299(6)
N(4)−C(2)	1.429(7)	N(2)−C(9)	1.413(7)
Mn(1)−N(3)−C(8)	148.9(5)	Mn(2)−N(1)−C(1)	142.3(4)
N(3)−C(8)−N(4)	174.4(5)	N(1)−C(1)−N(2)	177.1(6)
C(8)−N(4)−Mn(2)	111.2(3)	C(1)−N(2)−Mn(1)	111.7(3)
Mn(2)−N(4)−C(2)	128.6(3)	Mn(1)−N(2)−C(9)	132.5(3)
C(8)−N(4)−C(2)	116.0(4)	C(9)−N(2)−C(1)	115.8(4)

[a] Symmetry codes _a: $x, y-1, z$; _b: $x, y+1, z$; _e: $x, y, -z+1$; _f: $x, y, -z$.

or N(3)−Mn(1)−N(2) planes. Bridging phenylcyanamido ligands are far from planar, showing torsion angles for N(3)−N(4)−C(2)−C(3) of 38.7(4)° and N(1)−N(2)−C(9)−C(10) of 7.7(3)°.

In this case, a small deviation of the phenyl groups is evidenced by the 26.5(3)° or 0.8(3)° acute angles between the bond directions N(2)−C(9) or N(4)−C(2) with the reference $(NCN)_2$ plane. The Mn···Mn distance through the cyanamido unit is 5.407(1) Å, through the 4,4′-bpy bridge 11.712(1) Å, and the minimum interplane Mn···Mn distance is 10.289(1) Å.

Magnetic Measurements and Coupling Constant Calculations: Magnetic measurements were performed for compounds **2**−**4** in the 300−4 K temperature range on powdered crystalline samples, (see Exp. Sect.). The overall interaction is moderately antiferromagnetic in all cases.

The susceptibility plots increase gradually on cooling for compound **2** (Figure 7), but don't reach a maximum because at low temperatures a low quantity of impurities produce a sudden increase in the susceptibility value. The experimental data were analysed with the analytical expression for an isotropic $S = 5/2$ dinuclear compound by using the analytical expression derived from the isotropic Hamiltonian $H = -JS_1 \cdot S_2$, including an impurity term. The best fit parameters were $J = -3.5(1)$ cm^{-1}, $g = 2.01(1)$, $\rho = 0.030$.

Magnetic susceptibilities for compounds **3** and **4** also increase on cooling, reaching a broad maximum at 16 K in compound **4** (Figure 7). For compound **3** a sudden increase is also observed in the susceptibility values due to paramagnetic impurities. The coupling through the 4,4′-bpy bridges is negligible, so 2-D compound **4** should be assumed to be magnetically one-dimensional through the phenylcyanamido bridges. The experimental data were analysed with the analytical expression for an isotropic $S = 5/2$ chain system[7] derived by Fisher from the Hamiltonian $H = \Sigma -JS_i \cdot S_{i+1}$, including an impurity term for **3**. The best fit parameters were $J = -2.7(1)$ cm^{-1}, $g = 2.00(1)$, $\rho = 0.027$ and $J = -2.1(1)$ cm^{-1}, $g = 2.00(1)$ for **3** and **4,** respectively.

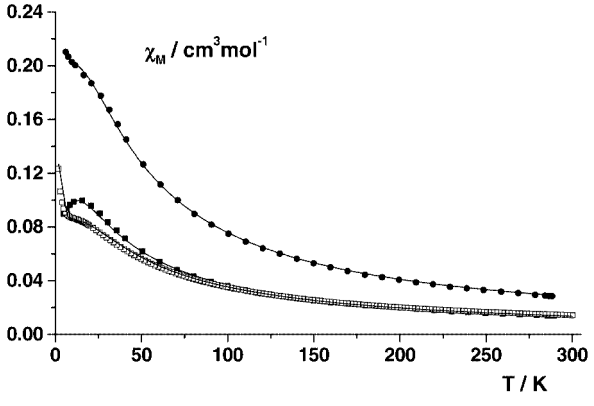

Figure 7. Plot of χ_M vs T for compounds [{Mn(pcyd)(phen)(MeOH)}$_2$($\mu_{1,3}$-pcyd)$_2$] (**2**) (solid circles) [Mn(4-bzpy)$_2$($\mu_{1,3}$-pcyd)$_2$]$_n$ (**3**) (open squares) and [Mn($\mu_{1,3}$-pcyd)$_2$(μ-4,4′-bpy)]$_n$ (**4**) (solid squares). Solid line shows the best fit of the data (see text)

EPR spectra for compound **1** show an isotropic broad band with a peak-to-peak increment (Δ_{pp}) of 674 G at room temperature, centred at $g = 2.00$. At 4 K the spectrum exhibits the main signal centred at $g = 2.00$ and a second weaker half-field band displaced at $g = 4.21$. Compound **2** shows one isotropic broad band at room temperature and 77 K, centred at room temperature at $g = 2.01$ with Δpp of 286 G. At 4 K the spectrum exhibits two main signals centred at $g = 2.01$ and 10.27 with Δpp of 438 G and 595 G, respectively, and several signals with minor intensities, which indicate some anisotropic effect at very low temperatures. Spectra of compounds **3** and **4** correspond nicely to that expected for one-dimensional systems with moderate antiferromagnetic coupling and weak dipolar interactions (Mn···Mn distances around 5.5 Å).[8] Between room temperature and 77 K the isotropic signals centered at $g = 2.01$ show a Δpp of 94 G and 92 G, respectively. Analogous Mn^{II} doubly bridged chains with end-to-end azido ligands with similar Mn···Mn intrachain distances have J values that typically lie around -10 cm^{-1}, the peak-to-peak linewidth being only 35 G due to the greater superexchange narrowing.[9] Instead, for weaker coupling, doubly dca bridged Mn^{II} chains, the peak-to-peak linewidth is much greater reaching values around 100−120 G[6] that show dipolar broadening on cooling down to 4 K.

The efficiency in transmitting the superexchange interactions is in the order $N_3^- > X\text{-pcyd}^- >> N(CN)_2^-$ [5] with typical values of the J parameter in the 1-D systems being around $-7/-15$ cm^{-1} (azido), $-1/-3$ cm^{-1} (X-pcyd$^-$) and weaker than -0.5 cm^{-1} for dicyanamide. The new series of J values reported here for the polynuclear phenylcyanamide bridged derivatives with Mn^{II} as the central atom confirms the assumption.

Conclusion

The ability of the X-phenylcyanamido ligands to act as bridging ligands has been newly confirmed by using the phenylcyanamido anion (pcyd$^-$) to synthesise a new series of formula [Mn(pcyd)$_2$(L)$_n$], L = phen, 4-bzpy and 2,2′-bpy, which show different nuclearities and dimensionalities. The coordination mode of the bridging pcyd$^-$ ligands is $\mu_{1,3}$. The magnetic measurements indicate AF coupling. The obtained coupling constant values are intermediate between the equivalent values for azido and dicianamido bridging ligands.

Experimental Section

Physical Methods: Magnetic susceptibility measurements were carried out on polycrystalline samples with a DSM8 pendulum susceptometer working in the range 4−300 K under magnetic fields of approximately 1 T. Diamagnetic corrections were estimated from Pascal tables. The infrared spectra (4000−400 cm^{-1}) were recorded from KBr pellets with a Nicolet 520 FTIR spectrophotometer. EPR spectra were recorded with a Bruker ES200 spectrometer at X-band frequency.

Table 5. Crystal data and structure refinement for $[Mn(pcyd)_2(phen)_2]$ (**1**), $[\{Mn(pcyd)(phen)(MeOH)\}_2(\mu_{1,3}\text{-pcyd})_2]$ (**2**), $[Mn(4\text{-bzpy})_2(\mu_{1,3}\text{-pcyd})_2]_n\cdot$MeOH (**3**·MeOH) and $[Mn(\mu_{1,3}\text{-pcyd})_2(\mu\text{-}4,4'\text{-bpy})]_n\cdot$MeOH (**4**·MeOH)

	1	**2**	**3**·MeOH	**4**·MeOH
Empirical formula	$C_{38}H_{26}MnN_8$	$C_{54}H_{44}Mn_2N_{12}O_2$	$C_{39}H_{32}MnN_6O_3$	$C_{25}H_{22}MnN_6O$
M_w	649.61	1002.89	687.7	477.43
Space group	Pbcn	*C*2/*c*	$P\bar{1}$	*C*2
a, Å	13.176(5)	15.758(6)	10.043(3)	18.498(4)
b Å	10.165(4)	13.771(4)	12.840(3)	11.712(2)
c, Å	23.530(8)	22.753(7)	14.448(5)	10.472(2)
α, deg.	90	90	112.29(2)	90
β, deg.	90	93.49(2)	90.96(2)	106.43(3)
γ, deg.	90	90	101.10(2)	90
V, Å^3	3151.5(20)	4928(3)	1683(1)	2176.0(7)
Z	4	4	2	4
T, °C	25(2)	−185(2)	−173(2)	−185(2)
λ(Mo-K_α), Å	0.71069	0.71069	0.71069	0.71069
$\rho_{calcd.}$, g·cm^{-3}	1.369	1.352	1.357	1.457
μ(Mo-K_α), mm^{-1}	0.461	0.567	0.440	0.638
R[a]	0.0486	0.0376	0.0522	0.0478
ωR^2[b]	0.1431	0.0926	0.1309	0.1197

[a] $R(F_o) = \Sigma F_o - F_c/\Sigma F_o$. [b] $\omega R\,(F_o)^2 = \{\Sigma[\omega[(F_o)^2 - (F_c)^2]^2]/\Sigma[\omega[(F_o)^4]\}^{1/2}$.

Synthesis: Neutral phenylcyanamide (pcydH) was prepared by desulfurisation of the phenylthiourea with lead acetate, following the described general synthetic procedure.[11]

Compound 1: 1 was prepared by reaction of a solution of manganese nitrate hexahydrate (1 mmol) and 1,10-phenanthroline (2 mmol) in 40 mL of methanol with a solution of pcydH (2 mmol) in 10 mL of NaOH (0.2 M) to deprotonate the ligand. After the reagents were mixed, the resulting clear solution was evaporated, giving a yellow crystalline compound suitable for X-ray measurements in a few days. Yield 21%. $C_{38}H_{26}MnN_8$ (649.6): calcd. C 70.3, H 4.0, N 17.2; found C 69.8, H 4.0, N 17.5.

Compound 2: 2 was prepared by reaction of a solution of manganese nitrate hexahydrate (1 mmol) and 1,10-phenanthroline (1 mmol) in 40 mL of methanol with a solution of pcydH (2 mmol) in 5 mL of NaOH (0.2 M) to deprotonate the ligand. After the reagents were mixed, the resulting clear solution was evaporated, giving a yellow crystalline compound suitable for X-ray measurements in three days. Yield 44%. $C_{54}H_{44}Mn_2N_{12}O_2$ (1002.9): calcd. C 64.7, H 4.4, N 16.8; found C 63.7, H 4.2, N 16.7.

Compounds 3 and 4: The method was the same as that for compound **2**, using 4-benzoylpyridine (2 mmol) for **3** and 4,4′-bipyridine (1 mmol) for **4** instead of phenanthroline (1 mmol). Yield of the corresponding yellow products, was 13% and 34%, respectively. Elemental analyses were performed on **3** and **4** in powdered samples three weeks after their preparation. **Compound 3:** $C_{38}H_{28}MnN_6O_2$ (655.6): calcd. C 69.6, H 4.3, N 12.8; found C 68.5, H 4.4, N 12.8. **Compound 4:** $C_{24}H_{18}MnN_6$ (445.4): calcd. C 64.7, H 4.1, N 18.9; found C 64.4, H 4.2, N 18.9. The elemental analysis for **3** and **4** indicates the absence of crystallisation of MeOH molecules in the powdered samples. To avoid errors in the magnetic measurements, the corresponding samples of **2** were freshly extracted from the mother solutions, dried and powdered just prior to performing the measurements. Moreover, the samples of **3** and **4** were dried and powdered some days before performing the magnetic measurements.

X-ray Crystallographic Study: Crystal data and details of the structure determinations are presented in Table 5. Data were collected on a modified STOE 4-circle diffractometer with graphite-monochromated Mo-K_α radiation (λ = 0.71069 Å) and the ω-scan technique. Data of **1**−**4**·MeOH were collected at room temperature, −185(2) °C, −173(2) °C and −185(2) °C, respectively, and processed in the usual way. The structures were solved by direct methods using the SHELXS-86 computer program,[12] and refined by full-matrix least-squares methods on F^2, using the SHELXL-93 program[13] incorporated in the SHELXTL/PC V 5.03 program library[14] and the graphics program PLUTON.[15] All non-hydrogen atoms were refined anisotropically. Hydrogen atoms bonded to donor atoms were located from difference Fourier maps, and the remaining ones were located on calculated positions by using the HFIX utility of the SHELXL-93 program. Selected bond parameters are given in Table 1−4 for compounds **1**−**4**·MeOH, respectively. CCDC-201204 (**1**), -201205 (**2**), -201206 (**3**·MeOH) and -201207 (**4**·MeOH) contain the supplementary crystallographic data for this paper. These data can be obtained free of charge at www.ccdc.cam.ac.uk/conts/retrieving.html [or from the Cambridge Crystallographic Data Centre, 12, Union Road, Cambridge CB2 1EZ, UK; Fax: (internat.) + 44-1223/336-033; E-mail: deposit@ccdc.cam.ac.uk].

Acknowledgments

A.E., R.V., and N.S. wish to thank the Ministerio de Ciencia y Tecnología (Spain), project BQU2000/0791 for the financial support to carry out this research. F.A.M. wishes to thank Prof. Belaj and Prof. Kratky (University of Graz) for the use of experimental equipment and OENB (project 7967) for financial support.

[1] J. Ribas, A. Escuer, M. Monfort, R. Vicente, R. Cortés, L. Lezama, L. T. Rojo, *Coord. Chem. Rev.* **1999**, *193*−*195*, 1027.
[2] [2a] A. Escuer, N. Sanz, F. A. Mautner, R. Vicente, *Inorg. Chem.* **2000**, *39*, 1668. [2b] P. M. Van der Werff, S. R. Batten, P. Jensen, B. Moubaraki, K. S. Murray, *Inorg. Chem.* **2001**, *40*, 1718. [2c] J. W. Raebiger, J. L. Manson, R. D. Sommer, U. Geiser, A. L. Rheingold, J. S. Miller, *Inorg. Chem.* **2001**, *40*, 2578. [2d] B. Vangdal, J. Carranza, F. Lloret, M. Julve, J. Sletten, *J. Chem. Soc., Dalton Trans.* **2002**, 566. [2e] A. Escuer, F. A. Mautner, N. Sanz, R. Vicente, *Inorg. Chim. Acta* **2002**, *340*, 163. [2f] P.

Jensen, S. R. Batten, B. Moubaraki, K. S. Murray, *J. Chem. Soc., Dalton Trans.* **2002**, 3712 and references cited therein.
[3] R. J. Crutchley, *Coord. Chem. Rev.* **2001**, *219−221*, 125.
[4] A. M. Galibert, O. Cortadellas, B. Soula, B. Donnadieu, P. L. Fabre, *J. Chem. Soc., Dalton Trans.* **2002**, 3743.
[5] A. Escuer, N. Sanz, R. Vicente, F. A. Mautner, *Inorg. Chem.* **2003**, *42*, 541.
[6] M. L. Brader, E. W. Ainscough, E. N. Baker, A. M. Brodie, *J. Chem. Soc., Dalton Trans.* **1990**, 2785.
[7] M. E. Fisher, *Am. J. Phys.* **1964**, *32*, 343.
[8] A. Bencini, D. Gatteschi, *EPR of Exchange Coupled Systems*, Springer-Verlag, Berlin, Heidelberg, **1990**, chapter 10, and references cited therein.
[9] M. A. M. Abu-Youssef, A. Escuer, D. Gatteschi, M. A. S. Goher, F. A. Mautner, R. Vicente, *Inorg. Chem.* **1999**, *38*, 5716.
[10] CACAO program (Computed Aided Composition of Atomic Orbitals), C. Mealli, D. M. Proserpio, *J. Chem. Educ.* **1990**, *67*, 399.
[11] B. R. Hollebone, R. S. Nyholm, *J. Chem. Soc., (A)* **1971**, 332.
[12] G. M. Sheldrick, SHELXS-86, Program for the Solution of Crystal Structure, University of Göttingen, Germany, **1986**.
[13] G. M. Sheldrick, SHELXL-93, Program for the Refinement of Crystal Structure, University of Göttingen, Germany, **1993**.
[14] SHELXTL 5.03 (PC-Version). Program library for the Solution and Molecular Graphics. Siemens Analytical Instruments Division, Madison WI, **1995**.
[15] A. L. Spek, PLUTON-92, University of Utrecht, 3584 CH Utrecht, The Netherlands, **1992**.

Received May 23, 2003
Early View Article
Published Online October 30, 2003